

# On the Wave Character of the Electron

G. Poelz\*

retired from Hamburg University  
Institute of Exp. Physics, Hamburg, Germany

## Abstract

A classical model of the electron based on Maxwell's equations is presented in which the wave character is described by classical physics. It uses a circulating massless electric charge field which moves in the spherical background of its own synchrotron radiation. A finite bound system exists which explains the features of the electron, and the wave character of this system yields a tight connection between the classical and the quantum mechanic world. The size of the object follows from the magnetic moment, and the finite synchrotron radiation requests a quantum mechanic core with a size determined via the angular momentum. The power of the synchrotron radiation yields the elementary charge i.e. the fine structure constant  $\alpha$ . Two circulations are required to obtain a stable circular orbit which is consistent with the description with the Dirac equation. The mass of the particle follows from the internal movement with speed of light. The system appears in the external world as a standing wave with an amplitude propagating like the de Broglie wave.

**Keywords** Electron · Classical wave model · Spherical wave field  
· Elementary charge ·  $\alpha$  · Mass · Wave character

## 1 Introduction

Electrical effects are known for several hundred years. The electron, as particle, has been discovered already at the end of the 19th century [1] and fascinates since then by its properties. It plays a fundamental role in the structure of matter, and in science like physics and chemistry. Today's technical designs are dominated by its applications.

The electron is perfectly described either on technical scales as a charged particle with its fields or in interactions at small distances by quantum mechanical computations. A common view is still missing.

The properties of the electron are summarized as follows:

- The electron has an elementary charge  $Q = -e$  with a point-like structure. This is expressed by an electric field which is described by the Coulomb field as a function of the distance  $r$  sketched in Fig. 1.

---

\*email: poelz@mail.desy.de

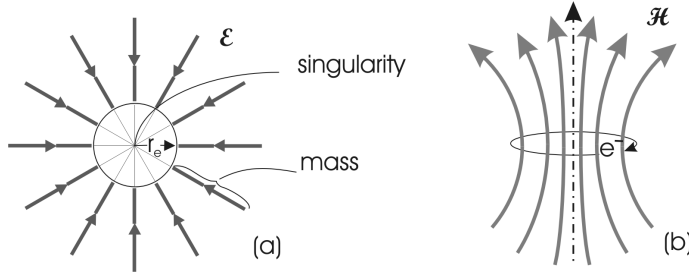


Figure 1: Classical picture of the electron. (a) The electric field points to the charge in the center. The Coulomb field is truncated at  $r_e$ , such that the residual field energy corresponds to the mass. (b) The magnetic moment of the electron suggests a current to be present.

$$\mathcal{E} = \frac{Q}{4\pi\epsilon_0 \cdot r^2} . \quad (1)$$

The problem of the singularity at the origin is usually removed just by a truncation at the so called “classical electron radius”  $r_e$ , by replacing the point charge by a charge distribution with radius  $r_e$ , or by modifying the electric permittivity  $\epsilon_0$  appropriately.

- It has a magnetic dipole moment

$$\mu = \frac{e}{2m_e} \cdot \frac{\hbar}{2} \cdot 2.0024 \quad (2)$$

which suggests a circulating charge like in Fig.1(b).

- The electron owns an intrinsic angular momentum, the spin, with

$$L_s = \frac{1}{2}\hbar . \quad (3)$$

- It has a finite rest mass

$$m_e = 9.11 \cdot 10^{-31} [kg] . \quad (4)$$

- It shows a wave like behavior at small distances defined 1924 by L. de Broglie [2] with a wave length  $\lambda$  related to its momentum  $p$  by

$$\lambda = \frac{2\pi\hbar}{p} . \quad (5)$$

- And from interactions at low and medium energies the Compton wavelength  $\lambda_C = h/m_e c = 2.43 \cdot 10^{-12} [m]$  emerges which describes the size of the particle.

The electron obeys the kinematic laws, and its electromagnetic interactions are perfectly described by Maxwell's equations and by their extensions to quantum mechanics. Many models have been built to describe the nature of this particle. The simplest ones in the classical region just attribute the rest mass of the particle to the electric field energy. It is common to truncate the field at  $r_e$  and call it the "classical electron radius".

$$r_e = \frac{e^2}{4\pi\epsilon_0 \cdot m_e c^2} = 2.8 \cdot 10^{-15} [m] . \quad (6)$$

With the assumption the electron is a surface charged sphere and the self energy is the mass energy one has to truncate the field at  $r_e^s$  or for a homogeneously charged sphere at  $r_e^h$ :

$$r_e^s = \frac{1}{2} r_e = 1.4 \cdot 10^{-15} [m] ; \quad r_e^h = \frac{3}{5} r_e = 1.7 \cdot 10^{-15} [m] . \quad (7)$$

But such a model with a specific charge distribution needs an artificial attractive force to compensate the electrostatic repulsion in the center [3] [4] [5] [6].

Many models exist which put the charge on a circular orbit or on a spinning top to explain spin and magnetic moment [7] [8] [9]. Special assumptions have always been necessary to cover most of the properties of the particle and special relativity leads to discrepancies if one associates the mass to the field energy of a massive electron [5] [6] [10].

The other approach to explain the electron structure comes from the wave mechanical side. The particle may be modeled by an oscillating charge distribution [3] or by the movement of toroidal magnetic flux loops [11]. Standing circular polarized electromagnetic waves on a circular path explain both the spin of the object as well as the electric field without a singular pointlike electric charge [12]. A massless charge on a Hubius Helix is described by arguments in analogy to the Dirac equation by Hu [13]. Spin, anomalous magnetic moment, particle-antiparticle symmetries are resulting.

With the spin of the electron in mind Barut and Zanghi [14] evaluated the Dirac equation for an internal massless charge. It lead to oscillations of the charge according to the Zitterbewegung predicted by the Dirac equation and detailed discussions on the relation between the Zitterbewegung and the helical structure of the electron have been done by Hestenes [15].

One is meanwhile accustomed to the view that classical mechanics and wave mechanics describe two different worlds, perfectly described for the electron by electrodynamics and by quantum electrodynamics with its extensions. A wide gap between both still exists which is not closed up to now by a satisfactory classical description.

The existing classical models deal with relativistic charges but disregard the generation of synchrotron radiation. Synchrotron radiation is dominant especially if one designs an electron by a circulating massless charge field and it turns out that this is a fundamental part of the electron.

It is the purpose of this paper to show that the electron may be described by an electromagnetic wave also in the classical region and thus a smooth transition between classical electrodynamics and quantum mechanics is established.

## 1.1 Outline

The electron will be described in the present paper by the dynamics of a massless charge. The creation of such a massless charge field e.g. by an annihilation of an electron-positron pair is visualized by the Feynman graph in Fig. 2. One expects that the high energy density at the interaction point leads immediately to quantum mechanical processes which decide on the particle family such as electron, muon or tau. There is still time of the order of  $h/m_e c^2 = 10^{-20} \text{ sec}$  for the electron to generate its elementary charge and its mass.

- First in this paper a massless charge field is considered which moves with speed of light on the most simple, a circular orbit to investigate its radiation.
- The synchrotron radiation of this charge is described by the *inhomogeneous* wave equation which is solved numerically.
- The resulting properties of angular momentum and radiation power give a first opportunity to compare these with the properties of the real electron.
- The solution of the *homogeneous* equation describes how the radiation propagates in space. An expression of this solution in spherical coordinates yields a background wave which propagates in azimuthal direction.
- The electric field lines within the spherical background field are investigated because they guide the charge through the radiation field.
- The conditions are investigated under which charge and radiation form a finite system which can be considered as the electron.
- The results on the properties of such an electron are discussed.

## 2 The Synchrotron Radiation of the Circulating Charge

In the Feynman diagram in Fig. 2 it is assumed that a massless charge pair was created. Such charges move with speed of light  $\beta = v/c = 1$ , will immediately be deflected by radiation processes, and may form central background fields in which they are bent onto circular paths.

The radiation of a charge is described by the solutions of the *inhomogeneous* wave equations for the electric potentials of the charge  $\vec{A}$  and  $\Phi$  e.g. expressed in Cartesian coordinates [16] with charge- and current-densities  $\rho$  and  $\vec{j}$ :

$$\begin{aligned} \Delta \vec{A} - \frac{1}{c^2} \frac{\partial^2 \vec{A}}{\partial t^2} &= -\mu_0 \vec{j}; \\ \Delta \Phi - \frac{1}{c^2} \frac{\partial^2 \Phi}{\partial t^2} &= -\frac{\rho}{\epsilon_0}. \end{aligned} \tag{8}$$

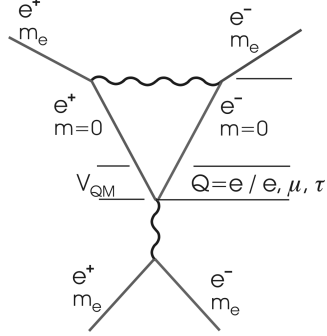


Figure 2: In this picture an electron-positron pair with masses  $m_e$  is annihilated at high energy and creates a virtual massless charge pair. The decision for either an  $e^-$ ,  $\mu^-$ , or a  $\tau^-$ -pair is made inside the quantum mechanics volume  $V_{QM}$  and within about  $t = h/m_e c^2 = 10^{-20}$  sec for an electron pair the elementary charges and the masses will then be formed.

The propagation of the radiation is described by the *homogeneous* wave equation. ( $\Phi = 0$  may be chosen)

$$\Delta \vec{A} - \frac{1}{c^2} \frac{\partial^2 \vec{A}}{\partial t^2} = 0. \quad (9)$$

This equation is discussed in section 3.

Solutions of the *inhomogeneous* equations for point-like charges are the retarded Liénard-Wiechert potentials [16] which are also valid at relativistic velocities

$$\Phi(\vec{r}, t, \vec{r}_Q, t_Q) = \frac{e}{4\pi\epsilon_0} \frac{1}{R - \vec{R} \cdot \frac{\vec{v}}{c}} \quad (10)$$

$$\vec{A}(\vec{r}, t, \vec{r}_Q, t_Q) = \frac{\mu_0 e}{4\pi} \frac{\vec{v}}{R - \vec{R} \cdot \frac{\vec{v}}{c}}. \quad (11)$$

An Observer  $P(\vec{r}, t)$  receives the fields from the circulating charge  $Q$  from an earlier position  $Q(\vec{r}_Q, t_Q)$  sketched in Fig. 3. The vector  $\vec{R}$  is given by  $\vec{R} = \vec{r} - \vec{r}_Q(t_Q)$  and  $\vec{v}$  is the velocity of the charge at the emission point. When the charge reaches  $Q_0$  at time  $t$  the length  $R$  is as long as the arc  $(Q, Q_0)$  for  $\beta = 1$ .

One computes the distance  $R$  between  $P(r, \vartheta, \phi, t)$  and the charge for each position of  $Q$ ,  $\varphi_Q$ ,  $\vartheta_Q = \pi/2$  in spherical coordinates by

$$R^2 = r^2 + r_Q^2 - 2rr_Q \sin \vartheta \cos(\phi - \phi_Q), \quad (12)$$

with

$$\begin{aligned} \phi_Q &= \omega \cdot t_Q, \quad t_Q = t - R/c \quad \text{and} \quad \omega = \beta c / r_Q \quad \text{one gets} \\ \phi - \phi_Q &= \phi - \omega t + \beta R / r_Q = \phi + \beta R / r_Q, \quad \text{with} \quad \phi = \phi - \omega t. \end{aligned} \quad (13)$$

One obtains

$$\frac{R^2}{r_Q^2} = \frac{r^2}{r_Q^2} + 1 - 2 \frac{r}{r_Q} \sin \vartheta \cos(\phi + \beta \frac{R}{r_Q}), \quad (14)$$

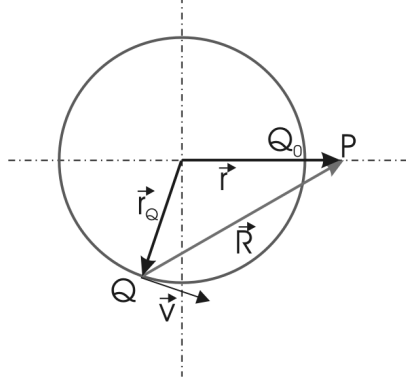


Figure 3: An observer at position  $P(\vec{r}, t)$  looks at the fields of a charge traveling on a circular orbit with velocity  $\vec{v}$ . He detects the fields which have been emitted at  $Q$  at an earlier time  $t_Q$ . For  $|\vec{v}| = c$  the distance  $R$  equals to the length of the arc  $(Q(t_Q), Q_0(t))$

and the component of  $\vec{R}$  along the velocity  $\vec{v}$  is then given by

$$R_v = \vec{R}\vec{v}/v = r \sin \vartheta \sin(\phi + \beta \frac{R}{r_Q}). \quad (15)$$

With these definitions the electric and magnetic fields

$$\vec{\mathcal{E}} = -\vec{\nabla}\Phi - \frac{\partial \vec{A}}{\partial t}; \quad \vec{\mathcal{H}} = \frac{1}{\mu_0} \vec{\nabla} \times \vec{A}. \quad (16)$$

are given by [16] .

$$\vec{\mathcal{E}} = \frac{e}{4\pi\epsilon_0} \left[ (1 - \beta^2) \frac{\vec{R} - R\vec{v}}{(R - \beta R_v)^3} + \frac{\vec{R} \times ((\vec{R} - R\vec{v}) \times \partial \vec{v} / \partial t_Q)}{c^2 (R - \beta R_v)^3} \right] \quad (17)$$

$$\vec{\mathcal{H}} = \epsilon_0 c \cdot \frac{1}{R} [\vec{R} \times \vec{\mathcal{E}}]. \quad (18)$$

and can be transformed to spherical coordinates with spherical components.

The first term in the brackets of equation (17) describes the field “attached” to the moving charge and the second term which contains the acceleration yields the radiation.

For a circular track in the horizontal plane the denominators of both terms become zero for  $\beta \rightarrow 1$ . The first term vanishes for points distant from the singular charge. The singularities of the fields in the second term arise when  $\vec{R}$  is tangential to the track i.e in the plane of the orbit. All singularities are located in this plane at  $R/r_Q = \sqrt{(r/r_Q)^2 - 1}$  at  $r \geq r_Q$ . They lead to huge energies close to these singularities and must result in quantum mechanical phenomena. With semi-classical arguments and Heisenberg’s uncertainty principle one expects the point charge to oscillate around its origin and generate on the average a finite charge distribution. The region of these singularities at  $\vartheta = \pi/2$  has to be excluded in classical considerations by appropriate cuts.

The second term shows how the charge field is embedded in its own synchrotron radiation. It will be shown that a circulating charge may generate a circulating electromagnetic wave to which it is bound. It is found that the interaction of a circulating

charge with its radiation field yields a solution with finite energy and angular momentum and forms a classical model of the electron.

One may compare this classical treatment with quantum mechanical descriptions of the electron. With the knowledge of the electron as a spin-1/2-particle it is described by the Dirac equation. One finds that the point like charge moves along circular or helical paths with a circumference given by the Compton wave length and is described as the “Zitterbewegung” (e.g. [14] [15]). Detailed discussions of the radiation are usually not done.

The evaluation of the radiation parts of the equations (17) and (18) in spherical coordinates yield the spherical components of the fields:

$$\mathcal{E}_r = \frac{e}{4\pi\epsilon_0} \frac{-\beta^2}{4rr_Q^2(R-\beta R_v)^3} \left[ \frac{[(R+r_Q)^2-r^2][(R-r_Q)^2-r^2]}{+4\beta r_Q^2 R R_v} \right] \quad (19)$$

$$\mathcal{E}_\vartheta = \frac{e}{4\pi\epsilon_0} \frac{-\beta^2}{4rr_Q^2(R-\beta R_v)^3} \frac{\cos \vartheta}{\sin \vartheta} \left[ 4\beta r_Q^2 R R_v - r^4 + (R^2 - r_Q^2)^2 \right] \quad (20)$$

$$\mathcal{E}_\phi = \frac{e}{4\pi\epsilon_0} \frac{\beta^2}{2rr_Q^2(R-\beta R_v)^3} \frac{r_Q}{\sin \vartheta} \left[ \frac{\beta R[R^2 - r_Q^2 + r^2(1 - 2\cos \vartheta^2)]}{-R_v(R^2 + r^2 - r_Q^2)} \right] \quad (21)$$

$$\mathcal{H}_r = \frac{ec}{4\pi} \frac{\beta^2}{2r_Q^2(R-\beta R_v)^3} [\beta r_Q \cos \vartheta (R^2 - r^2 + r_Q^2)] \quad (22)$$

$$\mathcal{H}_\vartheta = \frac{ec}{4\pi} \frac{\beta^2}{2r_Q^2(R-\beta R_v)^3} \frac{r_Q}{\sin \vartheta} \left[ \frac{\beta (R^2 + r^2 + r_Q^2) \cos \vartheta^2}{-2R(\beta R - R_v)} \right] \quad (23)$$

$$\mathcal{H}_\phi = \frac{ec}{4\pi} \frac{-\beta^2}{2r_Q^2(R-\beta R_v)^3} \frac{\cos \vartheta}{\sin \vartheta} [2\beta r_Q^2 R_v + R(R^2 - r^2 - r_Q^2)] \quad (24)$$

With these fields the following results are obtained.

## 2.1 The magnetic field

The massless circulating charge field on the circular track should behave like a classical circular current. Therefore the mean magnetic field of the charge field in the mid plane is compared with the magnetic field of a current loop with radius  $r_Q$  and a current of  $I = ec/2\pi r_Q$ . The magnetic fields were determined in the mid plane ( $\vartheta = \pi/2$ ) for  $r < r_Q$  and Fig. 4 shows that the crosses from the charge field are on top of the curve from the current.

## 2.2 The electric field of the radiation part

When for a circulating charge  $\beta$  approaches 1 the radiation term of equation (17) yields the dominant contribution to the electric field. The mean radial field should be equal to the Coulomb field, in the present case to the field of a charged ring.

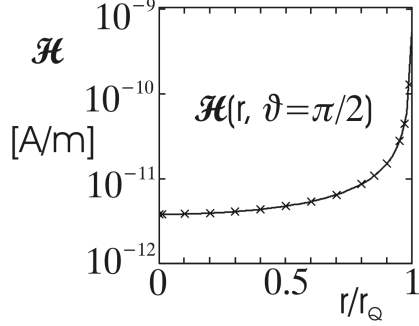


Figure 4: The size of the magnetic field in the plane of a circular current loop with a radius  $r_Q$  and with a current of  $I = ec/2\pi r_Q$  is shown as full line as a function of  $r$ . The values of the mean magnetic field of eq.(23) at  $\vartheta = \pi/2$  inside the circle are inserted as x-symbols and are on top of the curve.

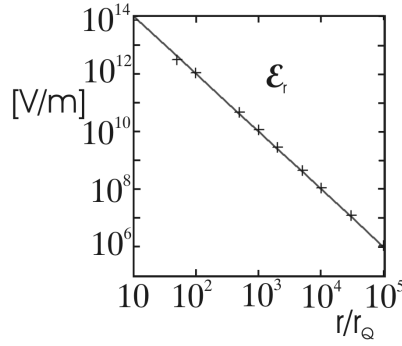


Figure 5: Comparison of the averaged electric field  $\mathcal{E}_r$  of a charge  $Q = +e$  circulating in the horizontal plane at a distance  $r_Q$  (+-signs) with a field of one in the center (full line) as a function of  $r$ .

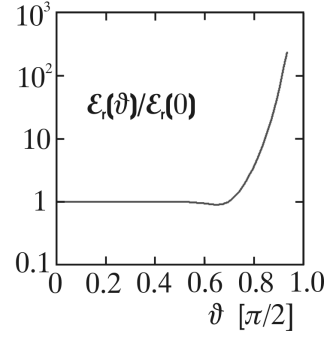


Figure 6: Radial electric field given by eq.(19) at  $r = 10^3 r_Q$  averaged over  $\phi$ , and normalized to the field at  $\vartheta = 0$ , as a function of the polar angle  $\vartheta$ .

The comparison of the electric field of two charges  $e$ , one circulating at a radius  $r_Q$  and one fixed at the center is made in Fig. 5. The full line represents the centered charge, and the +-signs come from the radial radiation field of the moving one given by eq.(19). The latter was averaged over the surface of the sphere with radius  $r$  over the interval  $[10^{-4} \leq \Delta\phi \leq 2\pi]$  with  $\Delta\phi$  the deviation of  $\phi$  from the singularity, and over  $[0.001 \leq \vartheta \leq 0.82\pi/2]$  (and symmetric to the mid plane).

The field is still not spherical symmetric at a distance of  $r = 10^3 r_Q$  as shown in Fig. 6. It is averaged there over  $\Delta\phi$  and normalized to that at  $\vartheta = 0$ , and is displayed as a function of  $\vartheta$ . It dominates close to the mid plane as expected.

### 2.3 The angular momentum of the radiation field

The fields of the radiation parts of eqs.(17) and (18) generate strong waves in azimuthal direction and thus cause an angular momentum. It depends on the azimuthal flux which is given by the Poynting Vector:



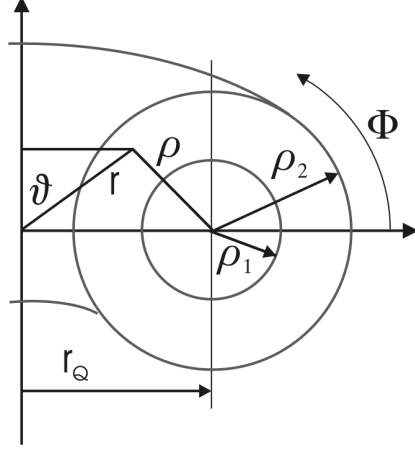


Figure 7: Sketch of the toroidal integration volume around the charge orbit.

$$\vec{\mathcal{J}} = \vec{\mathcal{E}} \times \vec{\mathcal{H}}. \quad (25)$$

At relativistic velocities it is directed into a narrow cone in forward direction at the circulating charge [16]. Its azimuthal component dominates close to the orbit and is seen at far distances as a radial component. It leads in technical devices to a permanent energy loss by radiation.

An electron model requires a constant energy which is performed by the reflection of the radial waves at the open end at infinity. These incoming waves are absorbed again by the circulating charge and provide a constant current. They form standing waves in radial direction and with the standing waves in  $\vartheta$ -direction only a mean flux in  $\varphi$ -direction is present.

For the last revolution of the charge moving with speed of light the azimuthal waves concentrate to regions close to the orbit. An observer at  $(r = r_Q, \varphi = 0)$  will see the field just on arrival time of the charge. But the radiation which was emitted by a charge at  $\varphi_Q = -2\pi$  reaches an observer at  $\varphi = 0$  at  $r = r_Q + 2\pi r_Q$  when this charge again arrives at  $\varphi = 0$ . This limits the volume in which the radiation should be investigated for one circulation.

The singularities in eqs.(19) to (24) show up also in the flux and have to be excluded. The angular momentum was therefore investigated in a toroidal volume with variable inner radius  $\rho_1$  as sketched in Fig. 7.

The angular momentum is then given by

$$L = \frac{1}{c^2} \int S_\varphi(\varphi, \rho, \Phi) r^2 \sin^2 \vartheta \rho d\rho d\Phi d\varphi \quad (26)$$

and is independent of the radius of the circulation  $r_Q$ .

The Poynting vector  $S_\varphi$  is computed at the observer and integrated from  $\rho_1/r_Q$  to the fixed outer border at  $\rho_2/r_Q = 1$  with cutting residual spikes. The angular momentum for one circulation of the charge in units of  $\hbar$  is plotted in Fig. 8 as a function of the inner radius  $\rho_1$ . One expects an angular momentum of  $1\hbar$ , or predicted by the Dirac equation of  $1/2\hbar$  but with two circulations. The respective values for  $\rho_1$  are

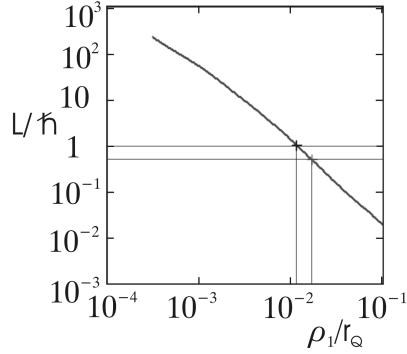


Figure 8: Angular momentum of the synchrotron radiation of an elementary charge moving on a circular path with radius  $r_Q$  with speed of light. The radiation was integrated in a toroidal tube sketched in Fig.7 from the variable inner radius  $\rho_1$  to  $\rho_2/r_Q = 1$ . The coordinates for  $L = \hbar$  and  $0.5\hbar$  are marked.

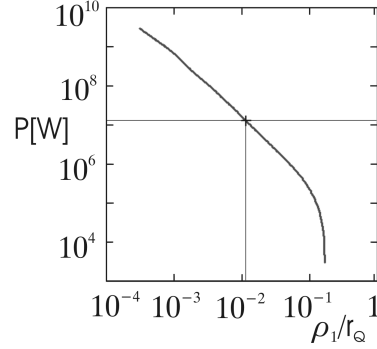


Figure 9: Power of the synchrotron radiation of the charge described and integrated like in Fig.8. At the inner radius  $\rho_1$  which was found for  $L = 1$  the power is  $1.2 \cdot 10^7 [W]$ .

$\rho_1(1) = (1.2 \pm 0.2) \cdot 10^{-2} r_Q$  and  $\rho_1(0.5) = (1.8 \pm 0.3) \cdot 10^{-2} r_Q$  and yield in this context the dimension of the quantum mechanic volume for all leptons.

## 2.4 The Power of the Synchrotron Radiation

The mean power of the emitted synchrotron radiation is given by the component of the Poynting vector  $S_\varphi$ . The components in  $r$ - and  $\vartheta$ -direction vanish on the average because of the standing waves in these directions. The power is then computed by

$$P = \frac{1}{r_Q^2} \int S_\varphi(\varphi, \rho, \Phi) \rho d\rho d\Phi \quad (27)$$

and averaged over all possible  $\varphi$ .

Again, the upper radius of the torus was fixed at  $\rho_2 = 1$  and the lower radius  $\rho_1$  was varied and residual spikes from the singularities were cut. The result is shown in Fig.9. At  $\rho_1(L = 1) = (1.2 \pm 0.2) \cdot 10^{-2} r_Q$  and with  $r_Q = 3.9 \cdot 10^{-13} [m]$  (s. next section) the power is  $(1.2 \pm 0.4) \cdot 10^7 [W]$ .

## 2.5 Interpretation and Comparison with Experimental Results

It was shown in Fig. 4 that the magnetic field of the charge field is equivalent to the current loop with  $I = ec/2\pi r_Q$ . From the experimental value of the magnetic moment

$\mu_e = 9.27 \cdot 10^{-24} [Am^2]$  and  $\mu = Ir_Q^2 \pi$  the radius of the circular path in the present model results then in

$$r_Q = 2\mu_e/ec = 3.86 \cdot 10^{-13} [m] \quad (28)$$

which determines the size of the electron, and the inverse we need later is calculated to

$$k = 2.59 \cdot 10^{12} [m^{-1}]. \quad (29)$$

The fundamental frequency is then

$$\omega = c/r_Q = 7.76 \cdot 10^{20} [s^{-1}] \quad \text{and its wavelength } \lambda = \frac{2\pi \cdot c}{\omega}. \quad (30)$$

A theory based on the Dirac equation leads to half of this wavelength but with two circulations [13] [15].

The singularities in the field equations (19) to (24) were removed by the argument that quantum mechanics leads to fluctuations in the position of the pointlike charge and generate a finite charge distribution. Its dimension was estimated via the angular momentum of the radiation which should be  $L = 1\hbar$  or  $0.5\hbar$ . Radii of

$$\begin{aligned} r_{QM} &= (1.2 \pm 0.2) \cdot 10^{-2} \cdot r_Q = (4.6 \pm 0.5) \cdot 10^{-15} [m] \quad \text{for } L = 1\hbar \text{ and} \\ r_{QM} &= (1.8 \pm 0.3) \cdot 10^{-2} \cdot r_Q = (7.1 \pm 0.1) \cdot 10^{-15} [m] \quad \text{for } L = 0.5\hbar \end{aligned}$$

were obtained. They are compatible with the cut-off radii  $r_e$  of  $1 \div 3 \cdot 10^{-15} [m]$  of section 1 but differ in their definitions. The radii  $r_e$  are computed with a static electrical field whereas the cut-off radii  $r_{QM}$  here are obtained in a dynamic environment.

The magnetic moment is usual expressed in quantum mechanic units:

$$\mu_e = 1.00116(e\hbar/2m_e). \quad (31)$$

The wavelength belonging to the fundamental frequency  $\omega$  expressed in these units becomes then

$$\lambda_e = 2\pi r_Q = 1.00116 \cdot h/m_e c, \quad (32)$$

which is just the Compton wavelength of the electron.

Quantum mechanics predicts the energy according to

$$E = \hbar\omega = 8.19 \cdot 10^{-14} [J], \quad (33)$$

which is consistent with mass energy  $m_e c^2$  of the electron.

Moreover the interaction of the electron with the photon results in the lowest angular momentum of  $L = 1\hbar$ . With the now traditional chain of arguments one gets (with radius  $r$ , energy  $E$ , circulation period  $T$ )

$$1\hbar = L = r \cdot p = r \cdot \frac{E}{c} = \frac{T}{2\pi} E. \quad (34)$$

The power of the radiation is

$$P = \frac{E}{T}, \text{ and leads to } 2\pi\hbar = \frac{E^2}{P}. \quad (35)$$

The synchrotron power for circulating electrons is dealt with in many text books on electrodynamics. A detailed elaboration by Iwanenko and Sokolov [24] is documented in section 6.1 and yields

$$P = \frac{e^2 \cdot c}{4\pi\epsilon_0 r_Q^2} \cdot Sum \quad (36)$$

Where *Sum* is the sum of integrals for the different contributing modes. For the fundamental mode  $n = 1$  only, one gets  $Sum = 0.5$  and e.g. the sum over  $n = 1 \div 20$  leads to  $Sum = 20$ . With  $P = 1.01 \cdot 10^7 [W]$  which corresponds to  $Sum = 22$  and which is close to the computed  $P = (1.2 \pm 0.4) \cdot 10^7 [W]$  one obtains the elementary charge

$$e = 1.6 \cdot 10^{-19} [C] \text{ or } \alpha = \frac{e^2}{4\pi\epsilon_0 \hbar c} = \frac{1}{137}. \quad (37)$$

It documents that the electron is a dynamic object.

From the reproduction of the experimental values with this simple picture of a charge moving on a circular path with  $\beta = 1$  one must conclude that solutions with a circular orbit dominate but many radiation modes contribute which will also be concluded in sections 3.4 and 3.5. Calculations with a charge distribution instead of a point charge should also provide values closer to reality.

### 3 The Solution of the Homogeneous Differential Equation

In the previous sections the charge was forced onto a circular track. It radiates permanently to balance its momentum and may only be stable if the emission of radiation is compensated by absorption. If this picture yields a model for the electron one must show that the massless orbiting charge embedded into the radiation field may move along stable tracks and that the whole electromagnetic object must be within a finite volume with finite angular momentum and finite energy.

The synchrotron radiation will now be investigated and the possible field lines which guide the charge will be determined.

The propagation of this radiation as any free electromagnetic radiation is described by the homogeneous differential equation, the wave equation (9).

The wave equation is usually solved in Cartesian coordinates in which the components separate and the subsequent transformation to cylindrical components allows for the investigation of multipole properties [17]. One is interested here in *spherical components* as considered with the inhomogeneous equations in section 2.

The wave equation in vacuum for the source free vector field  $\vec{A}$  in a spherical coordinate system which yields directly the spherical components has the form

$$\vec{\nabla} \times (\vec{\nabla} \times \vec{A}) + \frac{1}{c^2} \frac{\partial^2 \vec{A}}{\partial t^2} = 0 \quad (38)$$

The same equation is also valid here for the electric and magnetic fields  $\vec{\mathcal{E}}$  and  $\vec{\mathcal{H}}$ . (The substitution of  $\vec{\nabla} \cdot \vec{\nabla}$  by  $\Delta$  is only valid in a Cartesian coordinate system.)

If one writes  $\vec{A}$  as a product in spherical coordinates, e.g. for the space component

$$A_r = \mathcal{R}_r(x) \cdot \Theta_r(\vartheta) \cdot \Phi(\varphi) \cdot \mathcal{T}(t) \quad (39)$$

and with

$$\begin{aligned} \mathcal{T}(t) &= e^{\pm i\omega t} \quad \text{and} \\ \Phi(\varphi) &= e^{\pm im\varphi}, \quad k = \omega/c, \quad kr = x \end{aligned} \quad (40)$$

the wave equation separates in the coordinates, and one obtains equivalently 2 solutions also for both  $\vec{\mathcal{E}}$  and  $\vec{\mathcal{H}}$  which are interconnected via Maxwell's equations. (For details see the Appendix 6.2.)

### 3.1 Solution with standing waves

Special solutions, finite and smooth at the origin are obtained from the general solutions (Appendix eqs.(70) to (75)) with the Spherical Bessel functions of the 1<sup>st</sup> kind  $j_n(x)$  [18] [19]. They describe waves in  $\varphi$ -direction and have standing waves in  $x = kr$  and  $\vartheta$ . Their real parts yield one complete solution:

$$\mathcal{H}_r = 0 \quad (41)$$

$$\mathcal{H}_\vartheta = -C_k C_m e c k^2 (2m-1) P_{m-1}^{m-1}(\vartheta) j_m(x) \cos(m\varphi - kct) \quad (42)$$

$$\mathcal{H}_\varphi = C_k C_m e c k^2 P_m^{m-1}(\vartheta) j_m(x) \sin(m\varphi - kct) \quad (43)$$

$$\mathcal{E}_r = -\frac{C_k C_m e k^2}{\epsilon_0} (m+1) P_m^m(\vartheta) \frac{j_m(x)}{x} \cos(m\varphi - kct) \quad (44)$$

$$\begin{aligned} \mathcal{E}_\vartheta &= -\frac{C_k C_m e k^2}{\epsilon_0} \frac{P_m^{m-1}(\vartheta)}{2m+1} \cdot [(m+1)j_{m-1}(x) - m j_{m+1}(x)] \\ &\quad \cdot \cos(m\varphi - kct) \end{aligned} \quad (45)$$

$$\begin{aligned} \mathcal{E}_\varphi &= \frac{C_k C_m e k^2}{\epsilon_0} \frac{2m-1}{2m+1} P_{m-1}^{m-1}(\vartheta) \\ &\quad \cdot [(m+1)j_{m-1}(x) - m j_{m+1}(x)] \sin(m\varphi - kct). \end{aligned} \quad (46)$$

The  $P_n^m(\vartheta)$  are the Associated Legendre Functions, and the factors in front are chosen to give the right dimensions.  $C_k$  and  $C_m$  are normalization constants. The wave functions are unambiguous for  $m = 1, 2, 3, \dots$ , and the separation constant  $k$  determines the size of the whole object.

The second complete solution is the set in which the electric and magnetic fields are interchanged.

The general solution of this central wave is then a sum over all the harmonics  $m$  and over the wave numbers  $k$ , with the coefficients  $C_m$  and  $C_k$ , chosen to satisfy the boundary conditions. If this central wave should describe the propagation of the

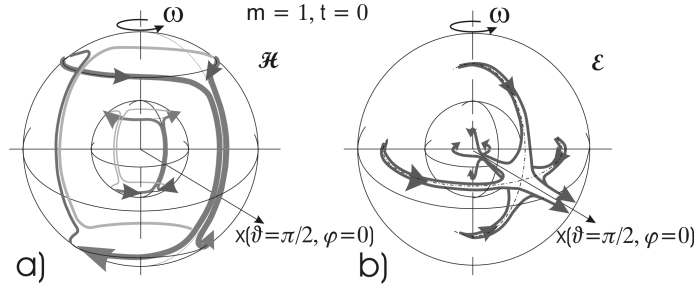


Figure 10: Sketch of typical field lines of the  $\mathcal{H}$ - and the  $\mathcal{E}$ -fields for  $m = 1$ . The spheres in a) on which the maxima of  $\mathcal{H}$  are located are also shown in b).

synchrotron radiation of a charge on the special circle assumed in chapter 2 then the dominating value of  $k$  is already fixed by eq.(29).

The discussion in section 2.5 suggests that solutions with  $L/\hbar = m = 1$  should dominate. These are mainly discussed here and the respective Bessel functions are:

$$\begin{aligned} j_0(x) &= \frac{1}{x} \sin x; & j_1(x) &= \frac{1}{x} \left[ \frac{1}{x} \sin x - \cos x \right]; \\ j_2(x) &= \frac{1}{x} \left[ \left( \frac{3}{x^2} - 1 \right) \sin x - \frac{3}{x} \cos x \right]. \end{aligned} \quad (47)$$

They decrease all with  $1/x$  and subdivide the fields into radial shells with alternating field directions from one to the next. A sketch of the fields  $\vec{\mathcal{H}}$  and  $\vec{\mathcal{E}}$  for  $m = 1$  for the innermost shells is displayed in Fig. 10.

### 3.2 The massless charge in the central wave

Now it will be investigated how the relativistic circulating charge behaves in the electromagnetic background field given by eqs.(41) to (46). A charge moving in the wave field with velocity  $\vec{v}$  sees an effective electric field  $(\vec{\mathcal{E}} + \mu_0 \vec{v} \times \vec{\mathcal{H}})$  which forces the charge to follow the field lines. This is possible by emitting radiation to balance the momentum.

To trace the field lines, a massless charge probe which moves with speed of light and which just follows the effective field was inserted and its track under different starting conditions was recorded. Such field lines were determined for waves with  $m = 1$ ,  $m = 2$ , and  $m = 3$  and for many starting points. A smooth field line has always been found for each condition and the field lines stayed in the mid plane if started there.

Especially simple field lines are obtained for  $m=1$  if started at  $\varphi = -\pi/2$  where the azimuthal electric field has a maximum. As an example four special closed field lines in the mid plane ( $\vartheta = \pi/2$ ) are drawn in Fig. 11. The axes are the Cartesian coordinates  $(\xi, \psi)$  of  $\vec{x}$ . There is the circular line with a radius of  $x = m = 1$ , the next one oscillates towards the center, and the next oscillates around  $x = 2$ . The one oscillating around  $x = 3$  shows counter rotating loops. These small loops become more and more flat

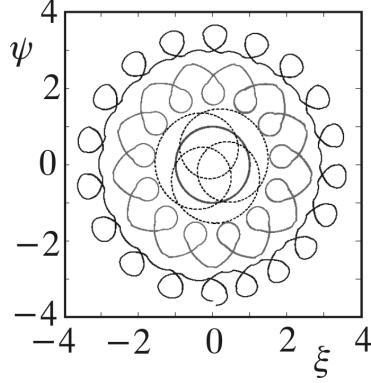


Figure 11: Four selected closed effective electric field lines in the central wave with Bessel functions of the 1<sup>st</sup> kind with  $m = 1$  seen by a charge moving with  $|\vec{v}| = c$ . The circular one has a radius of  $x = 1$ . The next, started at  $(\xi, \psi) = (0, -1.5)$  oscillates towards the center, one oscillates around  $x = 2$ , and the outer one at  $x = 3$  shows counter rotating loops. Shown is the mid plane  $\vartheta = \pi/2$  in Cartesian coordinates of  $(x, \vartheta, \varphi)$ :  $(\xi, \psi)$ .

for field lines further outward. The field lines can cross each other because they are functions of the coordinates and of the velocities as well.

A probe opposite in charge moving opposite to the origin finds the same field lines.

For waves with  $m = 2$  and higher the results differ due to the different symmetries and due to the phase velocity in azimuthal direction which is  $c$  at a radius  $x = m$ .

Smooth field lines have also been obtained outside the mid plain. They are similar to the ones already discussed but oscillate vertically.

One sees already how the system dynamically may behave: the charge will emit radiation to follow the field lines. This is a stochastic process and the resulting charge track will cross in general the azimuthal background wave. It will absorb then radiation energy until it moves again in the azimuthal direction.

### 3.3 Summation over harmonics and wave number

The Bessel functions decrease only with  $1/x$  which results in an infinite angular momentum and an infinite energy of the circulating wave in total space. A superposition of solutions with different  $m$  and different  $k$  might cure this problem in spite these parameters appear both in the Legendre Polynomials or in the Bessel functions and in the phase of the wave as well.

The angular momentum of the circulating wave integrated up to  $x = x_{max}$  is displayed in Fig. 12. It is independent of  $k$  and the momentum for  $m = 1$  only, with  $C_m = C_1 = 1$ , increases with  $x_{max}$  to infinity with periodic steps. If a Fourier like expansion in  $\varphi$  is applied to yield a finite result, already the addition of one counter rotating contribution with  $m = 3$  and the coefficients  $C_3/C_1 = 0.056$  leads to a constant but still oscillating result. An inclusion of terms with  $m = 2$  and  $m = 4$  had minor effects. Higher terms could not be tested because of the limited accuracy of the computing program.

The electric and the magnetic energy of the central wave sum up to a constant energy density  $dE/dx$  respective to  $x$  as displayed in Fig. 13 for  $m = 1$ . This would lead to an infinite total energy as expected from the Bessel functions.

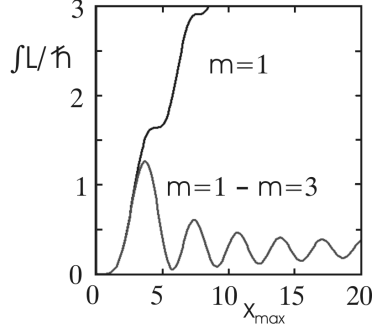


Figure 12: Angular momentum of the central wave in units of  $\hbar$  integrated up to  $x_{max}$ . The curve with “ $m=1$ ” displays the contribution with  $m = 1$  only. In “ $m=1 - m=3$ ” a counter rotating solution with  $m = 3$  is added.  $C_m = C_1 = 1$  and  $C_m = C_3 = 0.056$  were used (vertical axes unscaled).

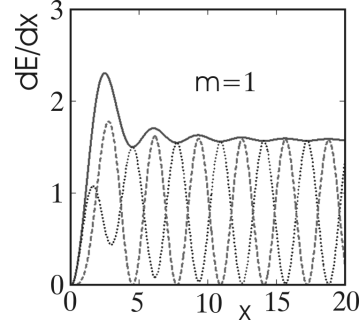


Figure 13: Energy density  $dE/dx$  of the electric ( $\cdots$ ) and the magnetic field ( $---$ ) of the central wave, and the sum of both (solid line) as a function of  $x$  for  $m = 1$  (vertical axes unscaled).

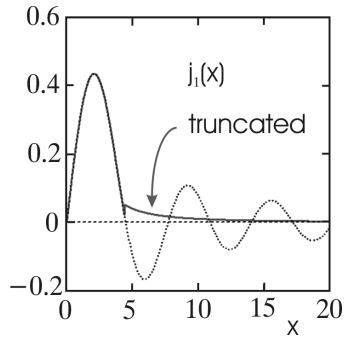


Figure 14:  $j_1(x)$  and the truncated function which was expanded in a Fourier-Bessel series.

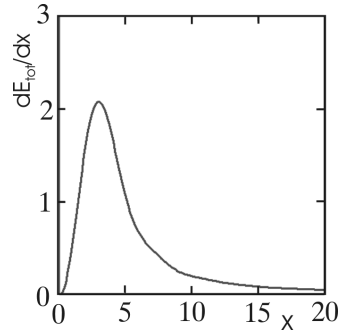


Figure 15: Total energy density  $dE_{tot}/dx$  after the replacement of  $k$  in the central wave by  $\lambda_i k$  and summed with coefficients obtained by the Fourier-Bessel expansion with the truncated function like in Fig. 14 .



Again an expansion is needed to obtain a finite value. The functions (41) etc. may be considered as members of a Fourier-Bessel expansion [20] [21]:

$$f(r) = \sum_i A_i j_m(k_i r) = \sum_i B_i j_m(\lambda_i x) \quad (48)$$

This may obviously be applied at  $t = 0$ . If e.g. for  $m = 1$   $j_1(x)$  in  $\mathcal{H}_\vartheta(x)$  is substituted by the truncated function shown in Fig. 14 and expanded in the region  $0 \leq x \leq 40$  the sum contains 12 terms. The expansion extended to all fields leads to reasonable results in spite of  $k$  occurs also in the wave part and in different Bessel functions. The resulting energy density shown in Fig. 15 would expect a finite total energy to be possible. Such a superposition would obviously also create a finite angular momentum.

These results show that solutions with stable and finite angular momentum and energy are possible but need in general a superposition of infinite terms i.e. infinite conditions.

### 3.4 Special solutions with Bessel functions

The investigation of the spherical waves was also extended to those with Spherical Hankel functions. They yielded however only simple field lines if 1<sup>st</sup> and 2<sup>nd</sup> Hankel functions with equal parameters were added i.e. if they are combined to Spherical Bessel functions of the 1<sup>st</sup> kind.

Especially simple field lines were found if the fields of eqs.(41) to (46) were combined with the 2<sup>nd</sup> solution in which  $\mathcal{H}$  and  $\mathcal{E}$  are interchanged and this inverted solution is shifted for  $m = 1$  by  $\Delta\varphi = \pm\pi/2$ .

The field lines approached always a horizontal circle around the center with radius  $x = 1$  but with constant vertical positions  $\zeta$  at about  $+1$  or  $-1$  for  $\Delta\varphi = -\pi/2$  or  $+\pi/2$  respectively. Both solutions combined average out to one with the circular field at  $\zeta = 0$ .

The sum of two such combinations with  $\Delta\varphi = \pm\pi/2$  shifted by  $\Delta\zeta = +1$  or  $-1$  respectively yielded such circular field lines now at  $\zeta = 0$  if they were started within a volume of about  $(\xi, \psi, \zeta) = (\pm 2, \pm 2, \pm 3)$ . This result would be compatible with a circular track in the mid plane described in section 2.

The graphs in Figs.16 and 17 are examples for such shifted combinations with  $|\Delta\zeta| = 1$  and for field lines started in the mid plane at the Cartesian coordinates  $\vec{x} = (0, -0.2, 0)$  and  $\vec{x} = (2.1, 2.1, 0)$  respectively.

When started above the mid plane at  $\vec{x} = (0, -1.5, 0.5)$  the circular line is approached exponentially as shown in Figs. 18 and 19.

Such centered circular field lines at  $\zeta = 0$  are also obtained for  $|\Delta\zeta|$  down to about 0.5. For  $0.2 \leq |\Delta\zeta| \leq 0.01$  the field lines form unknotted trefoils like the one in fig.11 but slightly bulged.

Corresponding results were obtained for  $m = 2$ . The field lines approached now a circle with radius  $x = 2$  when  $\Delta\varphi = \pi/4$ .

The superposition of two circulations is similar to the description with the Dirac equation in which the charge moves on a Hubius helix [13].

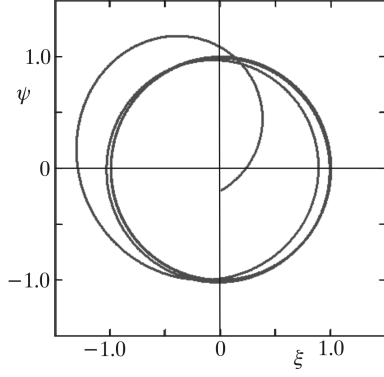


Figure 16: Effective electric field line in the central wave with Bessel functions for  $m = 1$ . To the fields of eqs.(41) to (46) the set with inverted  $\mathcal{E}$  and  $\mathcal{H}$  were added with a shift of  $\Delta\phi = +\pi/2$  and  $-\pi/2$  and the 2 pairs were displaced by  $\Delta\zeta = \pm 1$ . The field line was started at the Cartesian coordinates  $(\xi, \psi, \zeta) = (0, -0.2, 0)$  and moved to the circle with radius  $x = 1$ .

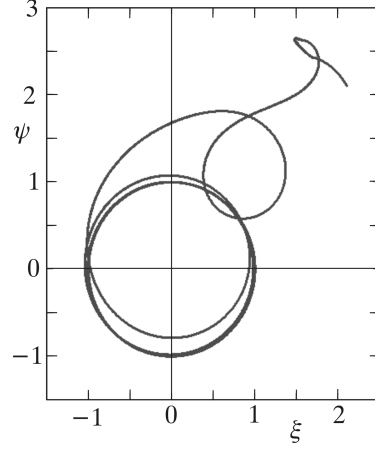


Figure 17: Field line like in Fig.16 but started at  $(2.1, 2.1, 0)$ .

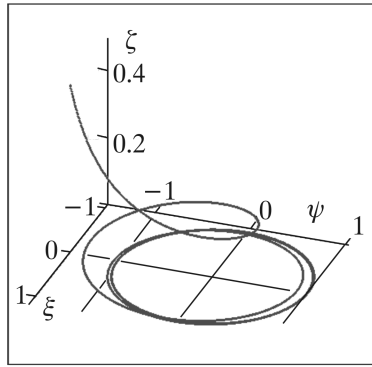


Figure 18: Field line in the central wave with Bessel functions like in Fig.16. The field line was started above the mid plane at  $(\xi, \psi, \zeta) = (0, -1.5, 0.5)$ .

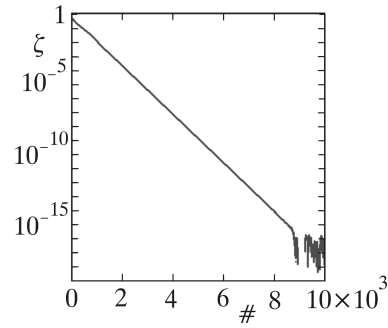


Figure 19: Vertical position of the field line of Fig.18 as a function of the step number of the simulation.

### 3.5 Angular momentum and energy.

In the configuration described in the previous section the massless charge is forced to follow the only possible track, the circular field line. Emission and absorption of radiation are concentrated there. The spherical background field thus will shrink towards the track of the charge which selects the appropriate superpositions in the solution and total angular momentum and total energy of the wave become finite. An extended simulation would be necessary to show the details.

## 4 On the Mass of the Electron

The electric field of a moving electron transports energy as well as momentum. The energy of the rest mass  $m_e c^2$  is generally assumed to equal the self-energy of a suitable charge distribution. The kinetic energy of a moving charge, on the other hand, yields different mass energies via the momentum calculated with the Poynting vector and via the energy of the magnetic field of the current. This is in contradiction to special relativity [4] [5] [10].

One expects that for a particle with the Cartesian coordinates  $(x_1, x_2, x_3)$  the energy transforms under Lorentz transformation e.g. in the  $x_1$ -direction like  $E^\beta = \gamma E$  and the momentum like  $(p_1^\beta, p_{2,3}^\beta) = (\beta \gamma p_1, p_{2,3})$  and  $E^{\beta^2} - (p^\beta c)^2 = E^2 - (pc)^2 = (mc^2)^2$  should yield the mass of the object. This is not true for the massive electron if one associates the mass with its field energy because energy and momentum of the field don't form a 4-vector. They belong to an energy-momentum tensor  $T_{\mu\nu}$  [22] [23] [25], with

$$\begin{aligned} T_{00} &= \rho^E = \frac{\epsilon_0}{2} \vec{\mathcal{E}}^2 + \frac{\mu_0}{2} \vec{\mathcal{H}}^2; \\ T_{0i} &= -\rho_i^P c = -S_i/c; \\ T_{ik} &= \epsilon_0 \left( \frac{1}{2} \vec{\mathcal{E}}^2 \delta_{ik} - \mathcal{E}_i \mathcal{E}_k \right) + \mu_0 \left( \frac{1}{2} \vec{\mathcal{H}}^2 \delta_{ik} - \mathcal{H}_i \mathcal{H}_k \right); \\ T_{\mu\nu} &= T_{\nu\mu}, \text{ and } i, k = 1 \dots 3, \mu, \nu = 0 \dots 3; \end{aligned} \quad (49)$$

$\rho^E, \rho_i^P$  are the energy and momentum densities of the field,  $\vec{S}$  is the Poynting vector, and  $T_{ik}$  Maxwell's stress tensor.

Lorentz transformation yields then the energy and momentum of a conventional charge moving with velocity  $v/c = \beta$

$$\begin{aligned} E^\beta &= \int \rho^{E\beta} d^3x^\beta \\ &= \frac{1}{\gamma} \int (\gamma^2 T_{00} + (\gamma^2 - 1) T_{11}) d^3x, \\ p_1^\beta c &= \int \rho_1^{P\beta} d^3x^\beta \\ &= -\beta \gamma \int (T_{00} + T_{11}) d^3x, \end{aligned} \quad (50)$$

$$\begin{aligned}
p_{2,3}^\beta &= \int \rho_{2,3}^\beta d^3x^\beta \\
&= -\beta \int (T_{12,3}) d^3x = 0,
\end{aligned}$$

and for the rest mass from energy and momentum squared

$$E^{\beta^2} - \vec{p}^{\beta^2} c^2 = \gamma^2 \left[ \int (T_{00} + \beta^2 T_{11}) d^3x \right]^2 - \beta^2 \gamma^2 \left[ \int (T_{00} + T_{11}) d^3x \right]^2. \quad (51)$$

Variables without the superscript  $\beta$  indicate that they apply to the rest frame.

In these equations neither the field energy nor its momentum show the proper dependence on  $\gamma$  and the rest mass is not constant. One might substitute the pointlike charge by a charge distribution at the origin of the electron to avoid the singularity of Coulomb's law [25]. But when a constant charge distribution is inserted inner forces result which have to be somehow compensated. One must require  $T_{11} = 0$  if eq.(51) should be valid at any particle speed.

The situation in the present model is different: The singularity is removed by the statistical oscillation of the point charge and this charge distribution moves with  $\beta = 1$ . The field energies are again the self energies now without the singularity. If one takes a differential section of the circular path where the charge moves in the 1-direction eq.(51) becomes now

$$\begin{aligned}
E^{\beta^2} - \vec{p}^{\beta^2} c^2 &= \gamma^2 \left[ \int (T_{00} + T_{11}) d^3x \right]^2 \\
&\quad - \beta^2 \gamma^2 \left[ \int (T_{00} + T_{11}) d^3x \right]^2 \\
&= \left[ \int (T_{00} + T_{11}) d^3x \right]^2.
\end{aligned} \quad (52)$$

This is constant and may be defined as the mass energy of the section, and integrated as the mass energy of the charge  $m_q c^2$ .

$$m_q c^2 = \frac{2q\epsilon_0}{3} \int \vec{\mathcal{E}}^2 d^3x \quad (53)$$

In addition there are the energy of the background wave  $E_w$  and an additional energy of the quantum mechanic center  $E_c$ . They all add to the total mass energy of the electron

$$m_e c^2 = m_q c^2 + E_w + E_c. \quad (54)$$

## 5 Conclusion

The presented investigations suggest that the classical electron can be described by a circulating massless charge field with its own synchrotron radiation included.

The circulating charge with  $\beta = 1$  is totally embedded in its own radiation field.

The Coulomb field is that of a charged ring and deviates from point symmetry at small distances.

The radius of the track is derived from the experimental value of the magnetic moment and is obtained to  $r_Q = 3.86 \cdot 10^{-13} [m]$ . It represents also the size of the object.

The values for the circulation frequency and the associated wavelength of the circular radiation, the Compton wavelength follow directly, and with Planck's constant  $\hbar$  the mass of the electron is obtained according to the definitions.

A small volume around the singularity of the charge fields has to be cut out. Quantum mechanical effects will dominate there, e.g. strong oscillations around the origin are expected which will result in a finite charge distribution there.

The angular momentum is carried by the radiation field. The contribution of the quantum mechanical volume should be small. The expected angular momentum of  $L = 1\hbar$  yields then the extension of the field and the size of inner volume to be cut. The radius of the quantum mechanical center is found to be  $(1.2 \pm 0.2) \cdot 10^{-2} \cdot r_Q = (4.6 \pm 0.5) \cdot 10^{-15} [m]$  compatible with the "classical electron radius"  $r_e$ . An angular momentum of  $L = 0.5\hbar$  connected with two circulations which is predicted by the Dirac equation yields a radius of  $(1.8 \pm 0.3) \cdot 10^{-2} \cdot r_Q = (7.1 \pm 0.1) \cdot 10^{-15} [m]$ .

The power of the synchrotron radiation with these cut-off radii in mind was determined to be  $(1.2 \pm 0.4) \cdot 10^7 [W]$ . With the theoretical power of  $1.01 \cdot 10^7 [W]$  one computes the elementary charge to  $e = 1.6 \cdot 10^{-19} [C]$  or  $\alpha = 1/137$ .

The mean electric field of the radiation part of eq.(17) reproduces the Coulomb field. The field is however not spherical symmetric but it dominates at short distances close to the plane of circulation as expected for a charged ring.

The solution of the *homogeneous* wave equation describes the propagation of the electromagnetic waves in vacuum. This background field may be formed during the creation process of the electron and be maintained by the synchrotron radiation of the charge. When evaluated in a spherical coordinate system it leads to a central background wave circulating in  $\phi$ -direction with a phase  $(m\phi \pm kct)$ .

A solution with Spherical Bessel functions of the 1st kind results in finite fields with standing waves in radial directions. Electric field lines in this wave seen by a charge moving with speed of light are smooth for each point and direction and may be suited to guide the charge. However the total angular momentum and the total energy of this radiation field are in general infinite over the whole space and the fields are not confined in the volume of the electron. Fourier like expansions with solutions summed over  $m$ , or  $x$  replaced by  $\lambda_i x$  and summed over  $\lambda_i$  show that finite solutions are possible.

If one solution is combined with the  $2^{nd}$  one in which the fields  $\vec{\mathcal{H}}$  and  $\vec{\mathcal{E}}$  are interchanged and the inverted one is shifted by  $\Delta\phi = +\pi/2$  or  $-\pi/2$  for  $m = 1$  the field lines approach always a circle with radius  $x = kr = 1$ . This circle is in the mid plane if 2 such pairs appropriately vertically shifted are combined. The charge will follow this circular field line and emission and absorption of radiation will concentrate at the track, and force the background wave to shrink close to the circle. The object will become finite. This resembles the prediction of the Dirac equation that two circulations are present.

The charge bucket moves with  $\beta = 1$ . The inner tensions which normally occur at

lower speed if one replaces the singularity by a constant charge distribution don't exist and a constant mass energy compatible with the relativistic energy-momentum tensor of the field results.

Thus one finds, that the electron may totally be described by a massless charge field embedded in its own synchrotron radiation. Radiation wave and charge are confined into a volume with the dimension of the Compton wave length and form a wave also in classical physics. Moreover this circular wave appears for an observer as a standing wave with frequency  $\omega = c/r_Q$  as described in section 6.3. When the particle moves with velocity  $\beta$  and momentum  $p$  the amplitude of the standing wave propagates like a wave with the phase velocity of  $v_{ph} = c/\beta$  as proposed by de Broglie [2]. This amplitude wave has a wavelength of  $\lambda = h/p$  and this discovery was the creation of wave mechanics.

The electron is a dynamic object. It does not only behave like a wave. It is a wave.

## 6 Appendix

### 6.1 Synchrotron radiation of the electron

A detailed discussion of the synchrotron radiation of the electron has been done by Iwanenko and Sokolov [24]. The radiated power of relativistic electrons in spherical coordinates for the  $n$ -th mode, circulation radius  $a$ , and Bessel functions  $J_n(z)$  is given by

$$dP_n = \frac{e^2 c \cdot \beta^2}{4\pi\epsilon_0 \cdot a^2} \cdot n^2 \left[ \cot(\vartheta)^2 \cdot J_n(z)^2 + \beta^2 \left( \frac{dJ_n(z)}{dz} \right)^2 \right] \sin \vartheta d\vartheta, \text{ with} \quad (55)$$

$$z = n\beta \sin \vartheta, \text{ and } \frac{d}{dz} J_n(z) = J_{n-1}(z) - \frac{n}{z} J_n(z). \quad (56)$$

For  $\beta = 1$ , integrated and summed over the equally weighted modes this leads to

$$P_n = \frac{e^2 c}{4\pi\epsilon_0 \cdot a^2} \cdot Sum_{nmax} \quad (57)$$

with

$$Sum_{nmax} = \sum_{n=1}^{nmax} n^2 \int_0^\pi \left[ \cot(\vartheta)^2 \cdot J_n(n \sin \vartheta)^2 + [J_{n-1}(n \sin \vartheta) - \frac{1}{\sin \vartheta} J_n(n \sin \vartheta)]^2 \right] \sin \vartheta d\vartheta. \quad (58)$$

Examples are:

$$Sum_1 = 0.45; \quad Sum_{20} = 19.5; \quad Sum_{100} = 105; \text{ etc.} \quad (59)$$

### 6.2 Solving the homogeneous wave equation in spherical coordinates

When the wave equation for a vector field  $\vec{\mathcal{F}}$

$$\vec{\nabla} \times (\vec{\nabla} \times \vec{\mathcal{F}}) = -\frac{1}{c^2} \frac{\partial^2 \vec{\mathcal{F}}}{\partial t^2} \quad (60)$$

is solved in spherical coordinates it yields directly the spherical components of the field. The equation separates in the variables when a product ansatz is made, e.g. for  $\mathcal{F}_r$ :

$$\mathcal{F}_r = A_r \cdot \mathcal{R}_r(x) \cdot \Theta_r(\vartheta) \cdot \Phi(\varphi) \cdot \mathcal{T}(t) \quad (61)$$

and with

$$\begin{aligned} \mathcal{T}(t) &= e^{\pm i\omega t} \quad \text{and} \\ \Phi(\varphi) &= e^{\pm im\varphi}, \quad k = \omega/c, \quad kr = x. \end{aligned} \quad (62)$$

One expects a source free wave field and one might subtract  $\vec{\nabla}(\vec{\nabla} \cdot \vec{\mathcal{F}})$  in eqn. (60). This simplifies the equation, but has to be checked afterwards. The ansatz eqn. (62) eliminates the time and  $\varphi$ -dependence and the 3 following components remain:

$$\left[ \begin{aligned} &-A_r \Theta_r(\vartheta) \frac{\partial}{\partial x} \frac{1}{x^2} \frac{\partial}{\partial x} x^2 R_r(x) \\ &-A_r \frac{R_r(x)}{x^2 \sin(\vartheta)^2} \Theta_r(\vartheta) (x^2 \sin(\vartheta)^2 - m^2) \\ &-A_r \frac{R_r(x)}{x^2 \sin(\vartheta)} \frac{\partial}{\partial \vartheta} \sin(\vartheta) \frac{\partial}{\partial \vartheta} \Theta_r(\vartheta) \\ &+A_\vartheta \frac{2R_\vartheta(x)}{x^2} \left( \frac{\cos(\vartheta)}{\sin(\vartheta)} \Theta_\vartheta(\vartheta) + \frac{\partial}{\partial \vartheta} \Theta_\vartheta(\vartheta) \right) \\ &+A_\varphi 2m \frac{R_\varphi(x)}{x^2 \sin(\vartheta)} \Theta_\varphi(\vartheta) \end{aligned} \right] = 0, \quad (63)$$

$$\left[ \begin{aligned} &2A_r R_r(x) \frac{\partial}{\partial \vartheta} \Theta_r(\vartheta) \\ &+A_\vartheta \Theta_\vartheta(\vartheta) \frac{\partial}{\partial x} x^2 \frac{\partial}{\partial x} R_\vartheta(x) \\ &+A_\vartheta R_\vartheta(x) \frac{\partial}{\partial \vartheta} \frac{1}{\sin(\vartheta)} \frac{\partial}{\partial \vartheta} \sin(\vartheta) \Theta_\vartheta(\vartheta) \\ &-A_\vartheta R_\vartheta(x) \Theta_\vartheta(\vartheta) \left( \frac{m^2}{\sin(\vartheta)^2} - x^2 \right) \\ &-2mA_\varphi R_\varphi(x) \frac{\cos(\vartheta)}{\sin(\vartheta)^2} \Theta_\varphi(\vartheta) \end{aligned} \right] = 0, \quad (64)$$

$$\left[ \begin{aligned} &2A_r R_r(x) \frac{m}{\sin(\vartheta)} \Theta_r(\vartheta) \\ &+2mA_\vartheta R_\vartheta(x) \frac{\cos(\vartheta)}{\sin(\vartheta)^2} \Theta_\vartheta(\vartheta) \\ &-A_\varphi \Theta_\varphi(\vartheta) \frac{\partial}{\partial x} x^2 \frac{\partial}{\partial x} R_\varphi(x) \\ &-A_\varphi R_\varphi(x) \frac{1}{\sin(\vartheta)} \frac{\partial}{\partial \vartheta} \sin(\vartheta) \frac{\partial}{\partial \vartheta} \Theta_\varphi(\vartheta) \\ &+A_\varphi R_\varphi(x) \Theta_\varphi(\vartheta) \left( \frac{m^2+1}{\sin(\vartheta)^2} - x^2 \right) \end{aligned} \right] = 0. \quad (65)$$

One obtains special solutions with the Spherical Bessel functions  $h_n(x)$  and the Associated Legendre functions  $P_n^m(\vartheta)$  if one chooses

$$R_{\vartheta}(x) = h_{n\vartheta}(x) + a_{\vartheta} \frac{h_{n\vartheta+1}}{x}(x) \quad (66)$$

$$\begin{aligned} R_{\varphi}(x) &= h_{n\varphi}(x) + a_{\varphi} \frac{h_{n\varphi+1}}{x}(x) \\ \Theta_r(\vartheta) &= P_p^q(\vartheta) \\ \Theta_{\vartheta}(\vartheta) &= P_v^{\mu}(\vartheta) \\ \Theta_{\varphi}(\vartheta) &= P_L^M(\vartheta) \end{aligned} \quad (67)$$

and uses

$$\begin{aligned} \frac{1}{\sin(\vartheta)} \frac{\partial}{\partial \vartheta} \sin(\vartheta) \frac{\partial}{\partial \vartheta} P_n^m(\vartheta) &= \left[ \frac{m^2}{\sin(\vartheta)^2} - n(n+1) \right] P_n^m(\vartheta), \\ \frac{\partial}{\partial x} x^2 \frac{\partial}{\partial x} h_n(x) &= [n(n+1) - x^2] h_n(x). \end{aligned} \quad (68)$$

If one eliminates  $R_r(x)$  from both eq. (64) and eq. (65), and sets  $R_{\vartheta}(x) = R_{\varphi}(x)$ , and  $q = m$  one arrives at

$$\left[ \frac{m P_p^m(\vartheta)}{\sin(\vartheta) \frac{\partial}{\partial \vartheta} P_p^m(\vartheta)} \cdot \left[ \begin{aligned} &-A_{\vartheta} \left( \frac{\partial}{\partial x} x^2 \frac{\partial}{\partial x} R_{\varphi}(x) \right) P_v^{\mu}(\vartheta) \\ &-A_{\vartheta} R_{\varphi}(x) \frac{\partial}{\partial \vartheta} \frac{1}{\sin(\vartheta)} \frac{\partial}{\partial \vartheta} \sin(\vartheta) P_v^{\mu}(\vartheta) \\ &+A_{\vartheta} R_{\varphi}(x) P_v^{\mu}(\vartheta) \left( \frac{m^2}{\sin(\vartheta)^2} - x^2 \right) \\ &+2A_{\varphi} m R_{\varphi}(x) \frac{\cos(\vartheta)}{\sin(\vartheta)^2} P_L^M(\vartheta) \end{aligned} \right] + \left[ \begin{aligned} &2mA_{\vartheta} R_{\varphi}(x) \frac{\cos(\vartheta)}{\sin(\vartheta)^2} P_v^{\mu}(\vartheta) \\ &-A_{\varphi} \left( \frac{\partial}{\partial x} x^2 \frac{\partial}{\partial x} R_{\varphi}(x) \right) P_L^M(\vartheta) \\ &+A_{\varphi} R_{\varphi}(x) \left[ \frac{m^2 - M^2 + 1}{\sin(\vartheta)^2} + L(L+1) - x^2 \right] P_L^M(\vartheta) \end{aligned} \right] \right] = 0. \quad (69)$$

One gets now 2 solutions for eq. (69). One for which both the upper and lower cluster vanish separately, and the other one for which the left side of this equation vanishes on the whole.

When these results are inserted into eq. (63) they determine  $R_r(x)$ , and  $\text{div}(\vec{\mathcal{F}}) = 0$  restricts the values of the separation constants. Both solutions may represent solutions of the electromagnetic fields  $\vec{\mathcal{E}}$  and  $\vec{\mathcal{H}}$  e.g.

$$\mathcal{H}_r = 0 \quad (70)$$

$$\mathcal{H}_{\vartheta} = C_H \cdot (2m-1) P_{m-1}^{m-1}(\vartheta) h_m(x) e^{(im\varphi - kct)} \quad (71)$$

$$\mathcal{H}_{\varphi} = i C_H \cdot P_m^{m-1}(\vartheta) h_m(x) e^{(im\varphi - kct)} \quad (72)$$

$$\mathcal{E}_r = C_E \cdot (m+1) P_m^m(\vartheta) \frac{h_m(x)}{x} e^{(im\varphi - kct)} \quad (73)$$



$$\mathcal{E}_{\vartheta} = C_E \cdot \frac{P_m^{m-1}(\vartheta)}{2m+1} \cdot [(m+1)h_{m-1}(x) - mh_{m+1}(x)]e^{(im\varphi - kct)} \quad (74)$$

$$\mathcal{E}_{\varphi} = iC_E \cdot \frac{2m-1}{2m+1} P_{m-1}^{m-1}(\vartheta) \cdot [(m+1)h_{m-1}(x) - mh_{m+1}(x)]e^{(im\varphi - kct)}. \quad (75)$$

The Bessel functions may either be of the  $1^{st}$ ,  $2^{nd}$ , or the  $3^{rd}$  kind [18] [19].

### 6.3 The de Broglie wave

Many textbooks refer to the de Broglie wave just by the citation of his relation  $\lambda = h/p$ . The derivation and a discussion is missing. He started from the existence of an internal clock in each particle and derived a wave with the wavelength  $\lambda$  connected with the particle speed  $p$ . His arguments are repeated here for completeness in the context of the classical model.

The internal structure of the electron in the present model is periodic in time e.g. in the laboratory frame with Cartesian coordinates  $(x_0, y_0, z_0, t_0)$  like

$$f_t = \cos(\omega_0 t_0) \quad \text{with} \quad \omega_0 = c/r_Q. \quad (76)$$

In addition the finite extension of the wave packet e.g. in  $x_0$  can be expressed by a Fourier expansion (or a Fourier integral) like

$$f_x = \sum_n A_n \cos(nk_0 x_0) + B_n \sin(nk_0 x_0) \quad (77)$$

Fluctuations in time and space are neglected.

Thus the wave packet may simplified be represented by the standing wave generated by plane waves

$$\Psi_0 = \cos(\omega_0 t_0) \cdot \sin(k_0 x_0). \quad (78)$$

Lorentz Transformation into a system  $(x, t)$  which moves with  $v_x = v$  is achieved by

$$\begin{aligned} x_0 &= \gamma \cdot (x - vt); & t_0 &= \gamma \cdot (t - \frac{\beta}{c} \cdot x); & y_0 &= y; & z_0 &= z; \\ \beta &= v/c; & \gamma &= 1/\sqrt{1 - \beta^2} & \text{and } \omega_0/k_0 &= c. \end{aligned} \quad (79)$$

and yields

$$\Psi = \cos(\omega_0 \gamma \cdot (t - \frac{\beta}{c} \cdot x)) \cdot \sin(\omega_0 \gamma \beta \cdot (\frac{x}{v} - t)). \quad (80)$$

The second factor represents the wave group. Its phase moves with the group velocity  $v_{gr} = dx/dt = v$ . The first factor may be considered as its amplitude whose phase moves with the phase velocity  $v_{ph} = dx/dt = c/\beta$ .

Quantum physics connects the energy with the frequency

$$E_0 = \hbar \omega_0; \quad E = \gamma E_0 = \hbar \omega, \quad \text{and with} \quad \beta = \frac{pc}{E} \quad (81)$$

one obtains

$$\Psi = \cos\left(\frac{E}{\hbar}t - \frac{p}{\hbar}x\right) \cdot \sin\left(\frac{E}{\hbar c}x - \frac{pc}{\hbar}t\right). \quad (82)$$

Comparison with the phase of a wave ( $\omega t - 2\pi/\lambda \cdot x$ ) yields the result of de Broglie that the amplitude behaves like a wave with:

$$\omega_{ph} = \frac{E}{\hbar} \quad \text{and} \quad \lambda_{ph} = \frac{h}{p}. \quad (83)$$

The charge in the present model is somewhere embedded in the wave with the probability of its location given by the amplitude.

The duration of an experiment in the view of the present model is determined by the arrival time of the wave packet and the interaction of the charge with an object.

## Acknowledgment

A presentation of an early version of this paper to E. Lohrmann showed the regions which have to be further deepened. I am grateful to K. Fredenhagen for many detailed discussions. Without the patience and the confidence of my wife Ursula this work would not exist.

## References

- [1] A. O. Barut, *Brief History and Recent Developments in Electron Theory and Quantumelectrodynamics*, in *The Electron: New Theory and Experiment* (D. Hestenes and A. Weingart, Editors; Springer, 1991) p. 105
- [2] L. de Broglie, *Nonlinear Wave Mechanics* (Elsevier, Amsterdam 1960) p. 6
- [3] P. A. M. Dirac, Proc. Roy. Soc. London **A268**, (1962) 57
- [4] J. D. Jackson *Classical Electrodynamics* (Wiley, New York 1975) §17.4
- [5] F. Rohrlich, Am. J. Phys. **65**, (1997) 1051
- [6] J. L. Jimenez and I. Campos, Found. Phys. Lett. **12**, (1999) 127
- [7] J. Orear, *Jay Orear Physics* (Macmillan, New York 1979) Chp. 18-4
- [8] M. Alonso, E.J. Finn, *Fundamental University Physics II* (Addison-Wesley, Amsterdam 1974) 515
- [9] M. H. McGregor, *The Enigmatic Electron* (Kluwer Academic, Dordrecht 1992)
- [10] A. Sommerfeld, *Electrodynamics: Lectures on Theoretical Physics* (Academic Pr., New York 1952) §33
- [11] H. Jehle, Phys. Rev. **D15**, (1977) p. 3727 and citations there.

- [12] J. G. Williamson and M.B. van der Mark, Ann. de la Foundation Louis de Broglie **22**, (1997) 133
- [13] Qiu-Hong Hu, Physics Essays, **17**, (2004) 442
- [14] A. O. Barut and N. Zanghi, Phys. Rev. Lett. **52**, (1984) 2009
- [15] D. Hestenes, Found. Phys. **20**, (1990) 1213
- [16] L. D. Landau and E. M. Lifshitz *The Classical Theory of Fields* (Butterworth-Heinemann, Oxford 2000) **2**, Chp. 8
- [17] J. D. Jackson [4] Chp. 16
- [18] *Handbook of Mathematical Functions* (editors: M. Abramowitz and I.A. Stegun; National Bureau Std., Appl. Math. Series 55, Washington 1966) Chp. 8, Chp. 10
- [19] P. M. Morse and H. Feshbach, *Methods of Theoretical Physics* (McGraw-Hill, New York 1953) Chp. 10, Chp. 11
- [20] I. N. Sneddon *Special Functions of Mathematical Physics and Chemistry* (Oliver and Boyd, Edinburgh 1961) §35
- [21] A. Sommerfeld, *Partial Differential Equations In Physics: Lectures On Theoretical Physics* (Academic Pr., New York 1952) §20, and exercise V.1
- [22] J. D. Jackson [4] Chp. 12
- [23] D. Iwanenko and A. Sokolov *Klassische Feldtheorie* (Akademie-Verlag, Berlin 1953) §29 - §30
- [24] D. Iwanenko and A. Sokolov *Klassische Feldtheorie* (Akademie-Verlag, Berlin 1953) §39ff
- [25] R. U. Sexl and H. K. Urbantke *Relativity, Groups, Particles* (Springer, Wien 2001) Chp. 5.10